

DESY 97-057
 April 1997

Cosmic Ray Constraints On the Annihilation of Heavy Stable Neutrinos in the Galactic Halo

Yu.A.Golubkov^{a)}, R.V.Konoplich^{b)}

^{a)} *Moscow State University, Moscow, Russia* ¹.

^{b)} *Moscow Engineering Physics Institute, Moscow, Russia* ².

Abstract

We carry out a detailed analysis of fluxes of cosmic ray antiprotons, positrons, electrons and photons to be expected from the annihilation of relic heavy neutrinos in the galactic halo. The spectra of particles are evaluated by Monte Carlo simulation. The results of calculations show that the investigation of cosmic ray positron spectra at high energies could provide a distinctive signal for annihilation of very heavy neutrinos in the Galaxy and give an important information on parameters of dark matter particles.

1 Introduction

The agreement that more or less exists between the observed and predicted abundances of light elements such as D , ${}^3\text{He}$, ${}^4\text{He}$ and ${}^7\text{Li}$ provides a confirmation of the standard cosmology and leads to the determination of the baryon density in the range [1]

$$\rho_B = (1.7 - 4.1) \cdot 10^{-31} \text{ g/cm}^3. \quad (1)$$

Because the critical density

¹e-mail: golubkov@elma01.npi.msu.su, golubkov@vxdesy.desy.de

²e-mail: konoplic@rosti.mephi.msk.su

$$\rho_c = 3H_0^2/8\pi G = 1.88 h^2 \cdot 10^{-29} \text{ g/cm}^3 \quad (2)$$

depends on the Hubble constant H_0 (h is the Hubble constant in units of $100 \text{ km s}^{-1} \text{ Mpc}^{-1}$) the present ratio of the baryon density of the Universe to its critical density also depends on H_0 ,

$$\Omega_B = \rho_b/\rho_c = (2.2 - 9.0) 10^{-2} h^{-2}. \quad (3)$$

Therefore for a wide range of the Hubble constant values, $h \approx (0.4 - 1)$, baryons contribute (1 - 15)% of the critical density of the Universe. Since the contribution of luminous matter

$$\Omega_{lm} \approx 3 \cdot 10^{-3} h^{-1} \quad (4)$$

is much less than 1% of the closure density, most baryons in the Universe should be dark either in the form of hot gas in clusters of galaxies or in the form of dark stars.

There are increasing observational evidences on a variety of scales favouring an average density of matter in the Universe which is significantly greater than 15% of the critical density possibly contributed by baryons. The non-Keplerian character of rotation curves around spiral galaxies indicates that they are at least ten times more massive than the sum of the stars which are being seen [2]. The velocity dispersion of stars and X-ray emission in elliptical galaxies show that these objects are also dominated by a dark component. At the scale of clusters of galaxies, independent sets of measurements point at an even greater amount of the dark matter. If this is the case, most of the matter in the Universe must be nonbaryonic. The evidence for dark matter in galaxies is collected in Ref.[3], and the evidence for dark matter in the Universe is summarized in Ref.[4].

Nonbaryonic dark matter can be divided into two broad classes on the basis of its clustering properties — the hot dark matter being relativistic at galaxy formation time and the cold one being slowly moving at that epoch. The most favoured hot dark matter candidate is a light neutrino with a mass $\sim 10 \text{ eV}$. Since light neutrinos are relativistic until relatively recent epochs, they would free-stream out off and damp out density perturbations up to the scale of galaxy clusters. However, the results from *COBE* show that the observed large scale structure cannot be explained with purely hot dark matter [5].

The cold dark matter on the another hand clusters at all scales, since it must have negligible free-streaming length. In the cold dark matter models, the structure generally forms hierarchically, with smaller clumps merging to form the larger ones. For this reason, theorists used to prefer the cold dark matter scenario over the hot one. But it is worth to note the recently surging popularity of the mixed scenario: a combination of 70% cold dark matter and 30% hot one produces a favourable spectrum of density perturbations and leads to consistency between the inflationary predictions and some dynamical estimations [6]. Theoretically, the favourite candidates for cold dark matter are the axion, an ultra-light pseudoscalar particle, and weakly interacting massive particles (WIMPS), with masses generally of the order of

100 GeV [7, 8]. The most attractive WIMPS candidate is the neutralino — a supersymmetric fermionic partner of the Standard Model bosons. For a review of the supersymmetric dark matter see [9]. In some models heavy neutrinos play also an important role in cosmology contributing part of the closure density [10, 11, 12].

The nature of the dark matter is certainly one of the most important questions facing both particle physics and cosmology. An indirect way to detect such dark matter particles is to study their signatures in cosmic rays.

In the present paper we carry out a detailed analysis of the influence of the annihilation of very heavy neutrinos ($m_\nu > 45 \text{ GeV}$) on cosmic ray production in the Galaxy. There exist a number of scenarios [13, 14] in which such very heavy neutrinos are expected to occur. To be explicit, we consider the standard electroweak model, including, however, one additional fermion family. The heavy neutrino ν and the heavy charged lepton L form a standard $SU(2)_L$ doublet. In order to ensure the stability of the heavy neutrino ν we assume that $m_\nu < m_L$ and that the heavy neutrino is a Dirac neutrino.

The organization of the paper is the following. In Sec.2 we discuss the residual relic number density of heavy neutrinos in the Universe and in the Galaxy. In Sec.3 we present various details of our calculations. In Sec.4 we discuss the results for the spectra of electrons, positrons, antiprotons and photons resulting from neutrino annihilation in the galactic halo and discuss signatures for the detection of heavy neutrino in cosmic rays. In Sec.5 we summarize the results of our analysis of cosmic ray spectra from neutrino annihilation. In the Appendix we present formulae for matrix elements of the reactions considered in the paper.

2 Relic number density of heavy neutrinos

It is known that the available experimental results do not preclude the existence of heavy Dirac neutrinos with masses $m_\nu > m_Z/2$ [15]. In the early Universe at high temperatures ($T \gg m_\nu$) such heavy neutrinos (if they exist) should be in thermal equilibrium with other species of particles. As the temperature in the Universe drops, heavy neutrinos become nonrelativistic at $T \sim m_\nu$ and their equilibrium concentration is proportional to $n_\nu \sim \exp(-m_\nu/T)$ [16]. However, in the further expansion of the Universe, as the temperature drops below the freeze-out value T_f , the weak interaction processes become too slow to keep neutrinos in equilibrium with other particles. As a consequence, the number density of heavy neutrinos fails to follow the equilibrium concentration (the exponential drop of the number density becomes much slower) reaching at present [18]:

$$n_\nu(T) \approx \frac{2 \cdot 10^{-18}}{\sqrt{g_*}} \frac{M_p}{m_\nu} \frac{1}{v_{rel} \sigma M_p^2} \left[40 + \ln \left(\frac{g_s}{\sqrt{g_*}} \frac{m_\nu}{M_p} v_{rel} \sigma M_p^2 \right) \right] n_\gamma(T), \quad (5)$$

where $n_\gamma(T) = 0.24T^3$ is the equilibrium photon number density, $T = 2.7 \text{ K}$ is the present photon temperature, M_p is the proton mass, v_{rel} is the relative $\nu\bar{\nu}$ velocity in units of

the velocity of light. The bar over quantity $v_{rel}\sigma$ means the averaging over the velocity distribution of the heavy neutrino.

The freeze-out temperature T_f can be found from the equation [16]:

$$\ln \left[\sqrt{\frac{m_\nu}{T_f}} \exp \left(\frac{m_\nu}{T_f} \right) \right] \approx 40 + \ln \left(\frac{g_s}{\sqrt{g_*}} \frac{m_\nu}{M_p} \overline{v_{rel}\sigma} M_p^2 \right), \quad (6)$$

In the above expressions g_s is the number of particle spin states (for photons and massive fermions $g_s = 2$). $g_*(T) = N_{bos} + \frac{7}{8}N_{ferm}$ is the number of effective degrees of freedom at given temperature (see [16]), N_{bos} is the number of bosons and N_{ferm} is the number of fermions (without heavy neutrinos) being in the thermal equilibrium at given temperature.

It was assumed in Eq.(5) that neutrinos are nonrelativistic at freeze-out, $T_f \ll m_\nu$. The numerical solution for Eq.(6) gives $T_f = 3.90 \text{ GeV}$ and $T_f = 10.7 \text{ GeV}$ for the heavy neutrino masses equal to $m_\nu = 100 \text{ GeV}$ and $m_\nu = 300 \text{ GeV}$, respectively. Thus, the non-relativistic approximation is valid. Therefore we can neglect the dependence of the annihilation cross section on velocity of the neutrino and in further calculations we take $\sigma(\sqrt{s}) = \sigma(2m_\nu)$. In this case we can replace $\overline{v_{rel}\sigma} \approx \overline{v_{rel}} \sigma(2m_\nu)$. Because $\overline{v_{rel}^2} = 2\overline{v^2}$ for definiteness in further calculations we can put $\overline{v_{rel}} = \sqrt{2}\overline{v}$, where $\overline{v} \approx 300 \text{ km} \cdot \text{s}^{-1}$ is the average velocity of heavy neutrinos in Galactic halo.

We have to note that Eq.(5) has been obtained using the analytical solution [16] for the expansion equation of hot equilibrium plasma. Such an approach gives correct order of magnitude, but, in principle, the equation has to be solved numerically to obtain more precise results. In the present paper we do not do this because our main aim is to show influence of the hadronization of final state quarks on the e^\pm , $p\bar{p}$ and γ fluxes as well as to correctly take into account energy losses for charged final state particles travelled through the Galaxy.

In the general case the following processes could lead to the annihilation of heavy neutrinos in the early Universe:

$$\nu \bar{\nu} \rightarrow \begin{cases} f \bar{f} & - s \text{ channel } Z^0, H^0 \text{ exchange} \\ W^+ W^- & - s \text{ channel } Z^0, H^0 \text{ and } t \text{ channel heavy lepton } L \text{ exchanges} \\ H^0 H^0 & - s \text{ channel } H^0 \text{ and } t \text{ channel heavy neutrino } \nu \text{ exchanges} \\ Z^0 Z^0 & - s \text{ channel } H^0 \text{ and } t \text{ channel heavy neutrino } \nu \text{ exchanges} \\ Z^0 H^0 & - s \text{ channel } Z^0 \text{ and } t \text{ channel heavy neutrino } \nu \text{ exchanges} \end{cases}$$

The annihilation of heavy neutrinos into a final state containing Z^0 boson or/and H^0 meson are suppressed in comparison with W^+W^- final state and will be neglected in the following consideration.

Qualitatively, the dependence of the present neutrino number density on its mass m_ν can be easily understood if one takes into account that neutrinos at freeze-out are nonrelativistic

and σ depends only on the mass of the heavy neutrino. The rate of “burning-out” of heavy neutrinos is proportional to the rate of collisions $N \sim v \sigma n_\nu^2$. Using Eq.(5) we obtain $N \sim 1/\sigma$ at $T \sim T_f$.

Thus the concentration of the heavy neutrinos at present, roughly speaking, depends inversely on its annihilation cross section. Therefore, in the region $m_\nu \sim M_Z/2$, the neutrino number density is extremely small as a result of the huge value of the annihilation cross section at the Z^0 boson pole. When the neutrino mass increases the cross section for neutrino annihilation into fermions drops and this leads to an increase of the neutrino number density, which reaches about $3 \cdot 10^{-10} \text{ cm}^{-3}$ at $m_\nu \sim 100 \text{ GeV}$. At $m_\nu > m_W$ the annihilation channel into W^+W^- opens and gradually becomes the dominant one since its cross section grows like m_ν^2 [17] and the present ν number density drops again. As it was shown in [18] the neutrino number density at $m_\nu > 2m_W$ is given, approximately, by

$$n_\nu \approx \frac{2 \cdot 10^{-9}}{(m_\nu/m_W) [(m_\nu/m_W)^2 + 4]} \text{ cm}^{-3}. \quad (7)$$

Above we discussed the neutrino number density in the Universe. However, at the stage of the formation of the Galaxy the motion of heavy neutrinos in the nonstatic gravitational field of ordinary matter, which contracts as a result of energy dissipation via radiation, provides an effective mechanism of energy dissipation for neutrinos [19]. As a consequence, the contracting ordinary matter induces the collapse of the neutrino gas and leads to the following significant increase in the neutrino density in the Galaxy [18, 19]:

$$n_{\nu G} \approx n_\nu \left(\frac{\rho_G}{\rho} \right), \quad (8)$$

where, $\rho_G \approx 5 \cdot 10^{-24} \text{ g/cm}^{-3}$ is the average density of matter in the Galaxy and $\rho \approx 4 \cdot 10^{-31} \text{ g/cm}^{-3}$ is the density of matter in the Universe.

3 Fluxes of particles from the heavy neutrino annihilation in the halo

The annihilation of dark matter particles in the galactic halo could produce detectable fluxes of elementary particles such as electrons, positrons, antiprotons and photons. For the case of supersymmetric dark matter particles a number of calculations of cosmic ray fluxes have been made (see, e.g., [20, 21, 22]). In this Section we present the results of our numerical calculations for fluxes of particles which appear either directly in the heavy neutrino annihilation or as secondary products of the fragmentation of quarks and gluons and from the decays of unstable particles.

Let us consider first the fluxes of electrons and positrons from heavy neutrino annihilation. In this case the differential spectrum of electrons (positrons) observable at the Earth is defined by [19]

$$J_e = \frac{\overline{v_{rel} \sigma}}{4 \pi} n_\nu^2 \frac{dn_e}{dE} v_e \tau_e, \quad (9)$$

where τ_e is the confinement time for electrons (positrons) in the galactic halo equal to $\tau_e \approx 10^7$ years and v is the interstellar $e^-(e^+)$ velocity. The quantity dn_e/dE is the energy spectrum of electrons produced in the annihilation of the heavy neutrino and antineutrino and normalized on one collision; n_ν is the present density of relic heavy neutrinos in the galactic halo.

In our calculations we assume that $\tau_e \approx 10^7$ years, but we have to note that the uncertainties here are substantial and can reach an order of magnitude. Moreover, τ_e can, in principle, depend on the initial energy of electron. Additional complications arise since the electrons (positrons) trapped in the galactic halo lose energy due to various processes. The energy losses for electrons and positrons propagating through the Galaxy halo matter are being defined by [20, 28]:

$$\frac{dE}{dt} = - \left[2.7 n_H + 7.3 n_H E + 1.02 (U_{rad} + U_{mag}) E^2 \right] \times 10^{-16} GeV s^{-1}, \quad (10)$$

where U_{rad} is the ambient photon energy density in $eV cm^{-3}$ and E is the $e^-(e^+)$ energy in GeV . The four terms in (10) represent the energy losses due to ionization of the H atoms, bremsstrahlung, inverse Compton scattering and synchrotron radiation in the galactic magnetic field, respectively. The electrons (positrons) spend most of their time, and lose most of their energy in the halo outside of the disc, where $n_H \sim 0.01 atoms cm^{-3}$, $U_{rad} \sim 0.25 eV cm^{-3}$ and $U_{mag} \sim 0.05 eV cm^{-3}$, so that inverse Compton scattering is dominant for $E \geq 1 GeV$. The e^- and e^+ spectra produced in neutrino annihilation must be corrected for these energy losses before the comparison with observations.

To calculate the particle fluxes from annihilation of very heavy neutrinos in the Galaxy we used the Monte Carlo approach. Such an approach allows to take into account the production of the particles of interest (e^+ , e^- , γ , p , \bar{p}) by hadronization of initial quarks or decays of heavier states. In this approach it is also easy to take into account the energy losses of final state electrons and positrons in the Galaxy.

Because we consider large masses of the heavy neutrino the resulting energies of final particles are also large, $E > 1 GeV$. In this case the dominant contribution comes from the two last terms in Eq.(10), which are proportional to E^2 , so that, $dE = -a E^2 dt$, where $a = 1.02 \cdot 10^{-16} (U_{rad} + U_{mag})$. Therefore, to simulate the broadening effect of energy losses we can use the distribution followed from the simple, spatially homogeneous model [28, 24]:

$$F(E, t) \sim \exp\left(-\frac{1}{a t E}\right), \quad (11)$$

which leads to:

$$E = \frac{E_0}{1 - 1.02 (U_{rad} + U_{mag}) 10^{-16} E_0 \tau_e \ln \xi}, \quad (12)$$

where E is the final energy of particle, E_0 is its initial energy and ξ is the random variable, with uniform distribution in the $(0, 1)$.

As it was mentioned in Sec.2 we restricted our consideration to the following two processes:

$$\begin{aligned} \nu + \bar{\nu} &\rightarrow f + \bar{f}, \\ \nu + \bar{\nu} &\rightarrow W^+ + W^-, \end{aligned} \tag{13}$$

where f denotes a lepton or a quark. The expressions for the differential cross section and matrix elements are given explicitly in the Appendix.

The simulation of the annihilation processes were performed with the package *PYTHIA 5.7* [27] with suitable modifications to include the fourth generation of fermions. To perform the hadronization and decays of final states we used the package *JETSET 7.4* [27]. This package is well tuned to the experimental data and gives a satisfactory description of final state multiplicities and particle distributions. We assumed that there is no mixing between the three light generations and the fourth one. For the hadronization of light quarks and gluons we used the symmetric LUND fragmentation functions and for heavy quarks the Peterson function. We also took into account the final state radiation in the annihilation reaction. This leads to a drastical increase of the spectra in the very low energy region. We have taken into account the decays of π , n and μ , which particles are usually considered to be stable. To avoid unnecessary complications we chose very high masses for the heavy lepton and Higgs $m_L = 1000 \text{ GeV}$, $m_H = 10000 \text{ GeV}$, because, as we have already mentioned previously, the Higgs contribution is important only in the resonance region $m_\nu \approx m_H/2$. We performed the simulation for two mass values of the heavy neutrino: $m_\nu = 100 \text{ GeV}$ and $m_\nu = 300 \text{ GeV}$ assuming for the mass of the t quark $m_t = 170 \text{ GeV}$. The other parameters have been left equal to their default values used in the *PYTHIA 5.7/JETSET 7.4* package (see for details [27]).

The results of our calculations for particle spectra are presented in Figs.3, 4 and for total cross sections in Table.1.

4 Discussion of numerical results

The results of the numerical simulation of the electron flux are presented in Fig.3(a) and in Fig.4(a) for $m_\nu = 100 \text{ GeV}$ and $m_\nu = 300 \text{ GeV}$, respectively, together with an approximation of the observable electron spectrum [23] of the type:

$$J_e^{exp} = 0.07 E^{-3.3} \text{ cm}^{-2} \text{ sr}^{-1} \text{ s}^{-1} \text{ GeV}^{-1}, \tag{14}$$

where E is $e^-(e^+)$ energy in GeV .

Without energy losses [18] we could expect a very narrow peak at $E_e = m_\nu/2$ with width $\Delta E_e \sim m v/c$ well above the background from the annihilation process $\nu \bar{\nu} \rightarrow e^+ e^-$ (since

heavy neutrinos in the Galaxy are nonrelativistic, $v \approx 300 \text{ km/s}$ is the velocity of neutrinos in the Galaxy) and from the continuum electron radiation resulting from decays of unstable particles. However, as we can see from Fig.3(a) and Fig.4(a), due to energy losses the resulting electron spectrum becomes significantly softer with a sharp edge at $E = m_\nu$. It appears that the electron spectrum cannot provide a clear signature for the heavy neutrino annihilation in the galactic halo.

As was noted in [18, 24] an important constraint on m_ν could be obtained by investigating the high energy part of the positron spectrum resulting from neutrino annihilation in the Galaxy. The flux of positrons from neutrino annihilation will be the same as in the case of electron production but the background conditions are significantly better. Up to now the positron flux has been measured only at energies $\leq 30 \text{ GeV}$. To estimate the expected positron flux at higher energies we performed a 3-parameter fit to experimental data for the $e^+/(e^+ + e^-)$ ratio in the form

$$R(E) = \frac{(a_1 + a_2 E)}{E^{a_3}}, \quad (15)$$

with three free parameters a_1, a_2, a_3 . The result of our fit is presented in Fig.1. In the energy region where separate measurements of electrons and positrons are available (see Fig.1) a significant excess of electrons has been found. At higher energies we can use either an extrapolation of our fit or the theoretical prediction. If we assume, for instance, the validity of the model of the dynamical halo, then the ratio e^+/e^- is found to be less than 0.02 at $E_e > 30 \text{ GeV}$ [23]. In this case we expect (see Fig.3(b)) a clear signature for heavy neutrino annihilation by an edge in the positron spectrum, which corresponds to the annihilation process $\nu \bar{\nu} \rightarrow e^+ e^-$. The detection of an excess of high energy positrons and a sharp edge of the positron spectrum (at $E = m_\nu$) would be a clear signature of the annihilation of Dirac neutrinos in the galactic halo [18, 24], since the direct annihilation of massive Majorana neutrinos into light fermions in the Galaxy is severely suppressed in the nonrelativistic case due to angular momentum conservation.

For the case $m_\nu = 300 \text{ GeV}$ the resulting electron spectrum is well below the background due to a sharp decrease of the neutrino number density when the neutrino mass increases above 100 GeV, $n_\nu \sim m_\nu^{-3}$.

The analysis of the \bar{p} spectrum is similar to that of electrons and is based on expression (9). However, it is important to note that in the case of antiprotons we can neglect their energy losses in the galactic disk due to mass suppression of synchrotron radiation and inverse Compton scattering in comparison with the case of electrons. Since antiprotons are trapped in the galactic magnetic field and have a rather large confinement time of the order 10^7 yr we can use the same expression (9) for an antiproton flux on the Earth which appears after a heavy neutrino annihilation and a sequential fragmentation of gluons and quarks. At low energies the ratio of antiprotons to protons in the cosmic rays is extremely low, namely less than about 10^{-4} for $E \sim 1 \text{ GeV}$ (see Fig.2). Therefore, if a sufficient amount of antiprotons was created in the hadronization process the antiproton flux can exceed the background and this could point at $\nu \bar{\nu}$ annihilation in the halo.

We present the results of our calculations of antiproton spectra in Figs.3(c), 4(c). We ignored a modulation of the antiproton flux due to solar wind effects in the region above 1 GeV. We took the interstellar cosmic ray proton spectrum to be [25]

$$J_p^{exp} = 1.93 \left(\frac{v_p}{c} \right) E_{kin}^{-2.7} \text{ cm}^{-2} \text{ sr}^{-1} \text{ s}^{-1} \text{ GeV}^{-1}. \quad (16)$$

where, $E_{kin} = E - M_p$ is a kinetic energy of the proton.

The dotted line shows our fit to the experimental data for the \bar{p}/p ratio (see Fig.2) (in the form as Eq.(15)) multiplied by the proton flux (16) for the region above 13 GeV. As it is seen, the antiproton signal is too small to be detected in the case of $\nu\bar{\nu}$ annihilation. Even if we compare our results with standard leaky box model prediction for the $\bar{p}p$ ratio $R_{LB} \approx 10^{-4}$ in the region 10 – 100 GeV the results are not favourable and cannot impose any significant constraint on the model.

Finally, we discuss the photon spectra resulting from $\nu\bar{\nu}$ annihilation. In the photon case there are no energy losses on the way to the Earth and the confinement time τ in eq. (9) is replaced by an integral over the line-of-sight which depends on the galactic latitude b and longitude l [29, 20]:

$$J_\gamma^{exp} = \frac{\overline{v_{rel} \sigma}}{4\pi} n_\nu^2 \frac{dn_\gamma}{dE} a I(b, l), \quad (17)$$

where for the diffuse γ component factor $I(b, l) \approx 1.24$ (high galactic latitudes) and $a \approx 10 \text{ kpc}$. The diffuse photon background is not known for $E_\gamma > 1 \text{ GeV}$. Using data from the MeV region and extrapolating to higher energies, the photon spectrum is inferred to be [22]

$$J_\gamma^{exp} = 8 \cdot 10^{-7} E_\gamma^{-2.7} \text{ cm}^{-2} \text{ sr}^{-1} \text{ s}^{-1} \text{ GeV}^{-1}. \quad (18)$$

The results of our γ calculations are shown in Fig.3(d) and Fig.4(d). As we see in the case of $m_\nu = 100 \text{ GeV}$ the neutrino annihilation leads to an indirect production of photons through particle decays above the expected background. However it seems that the continuous photon spectrum is not sufficient to give us a clear signature of the neutrino annihilation in the galactic halo. The difference between the predicted spectrum and the expected background is not very significant and the flux is small.

We should note that our calculations contain significant uncertainties in astrophysical assumptions especially about the laws of propagation for \bar{p} and e^+ in the Galaxy and the local halo density.

5 Conclusion

In this paper we have carried out a detailed analysis of fluxes of cosmic ray antiprotons, positrons, electrons and photons to be expected from the annihilation of relic heavy stable

neutrinos in the galactic halo. We used the standard electroweak model including one additional fermion family and the idea of neutrino condensation in the gravitational field of collapsing matter at the stage of Galaxy formation. Our conclusion is that it is difficult on the basis existing experimental data on cosmic ray spectra to constrain parameters of heavy neutrinos. However, it seems that future experimental study of cosmic rays and especially their e^+ and γ components in the high energy region, could give important information on dark matter particles. In particular the detection of the anomalous positron output corresponding to the monochromatic annihilation line at the edge of the positron spectrum would be a clear indication for the annihilation of Dirac particles of dark matter in the galactic halo. Also the investigation of the continuum spectrum of diffuse γ rays above 1 GeV could be used in order to constrain the parameters of dark matter particles or to provide a confirmation of a signal seen in other experiments. As it was mentioned in [20] a possible strategy for future experiments is to combine positron detection with those for antiprotons and photons.

Note that direct detection experiments [34] using semiconductor ionization detectors excluded heavy Dirac neutrinos as a major component of our galactic halo in the mass region 10 – 1000 GeV . However, the investigation of cosmic ray spectra could play an important role in the case of multicomponent dark matter and may be used for species (in particular, neutrinos) that give a negligible contribution to the total energy density of the Universe.

We also emphasize the possibility of searching for very heavy neutrinos in accelerator experiments by the process $e^+e^- \rightarrow \nu\bar{\nu}\gamma$ [35] which allows investigation in the region $m_\nu \sim m_Z/2$, where it is extremely difficult to get cosmological constraints on neutrino masses due to a very low neutrino number density in this mass region. If heavy neutrinos exist there could be also an interesting hadronless signature for Higgs meson strahlung production at accelerators $e^+e^- \rightarrow Z^0 H^0 \rightarrow Z^0 \nu\bar{\nu} \rightarrow l^+l^- \nu\bar{\nu}$ and this mode could be the dominant one.

Acknowledgement

It is a pleasure to thank Prof. G.Wolf for careful reading of the manuscript and very useful remarks and comments and Prof. M.Yu.Khlopov for valuable conversations.

One of the authors (Yu.G.) wants to express his gratitude to DESY for support during the preparation of this work for publishing.

Table.1. Total cross sections.

	$m_\nu = 100 \text{ GeV}$ $T_f = 3.90 \text{ GeV}$	$m_\nu = 300 \text{ GeV}$ $T_f = 10.6 \text{ GeV}$
Final state	$\sigma_{tot}, (nb)$	$\sigma_{tot}, (nb)$
$d\bar{d}$	3.30	0.245
$u\bar{u}$	2.50	0.189
$s\bar{s}$	3.16	0.245
$c\bar{c}$	2.52	0.192
$b\bar{b}$	3.26	0.287
$t\bar{t}$	—	40.0
e^-e^+	0.737	0.0554
$\nu_e\bar{\nu}_e$	1.48	0.110
$\mu^-\mu^+$	0.743	0.0554
$\nu_\mu\bar{\nu}_\mu$	1.48	0.110
$\tau^-\tau^+$	0.724	0.0571
$\nu_\tau\bar{\nu}_\tau$	1.48	0.110
W^+W^-	16.2	121
Σ over all channels	36.2	162

References

- [1] *C.J.Copi, D.N.Schramm and M.S.Turner.* Science **267** (1995) 192.
- [2] *M.Fich and S.Tremane.* Annu. Rev. Astron. Astrophys. **29** (1991) 409.
- [3] *K.M.Ashman.* Proc. Astron. Soc. Pac. **104** (1992) 1109.
- [4] *V.Trimble.* Annu. Rev. Astron. Astrophys. **25** (1989) 425.
- [5] *L.Blitz,* in: Dark Matter, Proc. 5th Annual October Astrophysics Conference in Maryland: International Conference on Dark Matter, College Park, MD, 10–12 Oct. 1994, eds. S.S.Holt and C.L.Bennett (American Institute of Physics, New York, 1995).
- [6] *J.A.Holtzman.* Astrophys.J. Suppl. **71** (1989) 1; *M.Davis, F.J.Summers and D.Schlegel.* Nature **359** (1992) 393; *J.R.Prymack and J.A.Holtzman.* Astropys.J. **405** (1993) 428; *A.Klypin et al.* Astrophys.J. **416** (1993) 1.
- [7] *M.S.Turner.* Phys. Rep. **197** (1990) 67.
- [8] *G.Raffelt.* Phys. Rep. **198** (1990) 1.
- [9] *G.Jungman, M.Kamionkowski and K.Griest.* Phys. Rep. **267** (1996) 195.
- [10] *M.I.Vysotski, A.D.Dolgov and Ya.B.Zel'dovich.* JETP Lett. **26** (1970) 188.

- [11] *B.W.Lee and S.Weinberg.* Phys. Rev. Lett. **39** (1977) 165.
- [12] *P.Hut.* Phys.Lett. **B69** (1977) 85.
- [13] *C.T.Hill and E.Paschos.* Phys.Lett. **B241** (1990) 96.
- [14] *A.Datta and S.Raychaudhuri.* Phys.Rev. **D49** (1994) 4762.
- [15] *Review of Particle Physics.* Phys.Rev. **D54** (1996) 1.
- [16] *A.D.Dolgov and Ya.B.Zeldovich.* Rev.Mod.Phys. **53** (1981) 1.
- [17] *K.Enquist, K.Kainulainen and J.Maalampi.* Nucl.Phys. **B317** (1989) 647.
- [18] *D.Fargion, M.Yu.Khlopov, R.V.Konoplich, R.Mignani.* Phys.Rev. **D52** (1995) 1828.
- [19] *Ya.B.Zeldovich, A.A.Klypin, M.Yu.Khlopov and V.M.Chechetkin.* Sov.J.Nucl.Phys. **31** (1980) 664.
- [20] *J.Ellis, R.A.Flores, K.Freese, S.Ritz, D.Seckel and Joseph Silk,* Phys. Lett. **214B** (1988) 403.
- [21] *G.Jungman and M.Kamionkowski,* Phys.Rev. **D49** (1994) 2316.
- [22] *E.Diehl, G.L.Kane, C.Kolda and J.D.Wells,* Phys.Rev. **D52** (1995) 4223.
- [23] *D.Mueller and Kwok-kwong Tang,* Astrophys.J. **312** (1987) 183.
- [24] *M.S.Turner and F.Wilczek.* Phys.Rev. **D42** (1990) 1001.
- [25] *M.J.Ryan, F.Ormes and V.K.Balasubrahmanyam.* Phys.Rev.Lett **28** (1972) 985.
- [26] *The Wizards Collaboration.* Phys.Rev.Lett. **75** (1995) 3792; Preprint INFN-AE-95-22. See also references therein for observed \bar{p}/p and $e^+/(e^+ + e^-)$ cosmic ray flux ratios.
- [27] *T.Sjöstrand.* Comp. Phys. Comm. **82** (1994) 74.
- [28] *M.S.Longair,* in: High energy astrophysics (Cambridge U.P., Cambridge, 1981) p.278.
- [29] *J.E.Gunn et al,* Astrophys. J. **223** (1978) 1015; *M.S.Turner,* Phys. Rev. **D34** (1986) 1921.
- [30] *B.Agriner et al.* Lett. Nuovo Cim. **1** (1969) 53.
- [31] *A.Buffington et al.* Astrophys.J. **199** (1975) 669.
- [32] *J.L.Fanselow et al.* Astrophys.J. **158** (1969) 771.
- [33] *R.L.Golden et al.* Astron. Astrophys. **188** (1987) 145.
- [34] *S.P.Ahlen et al.* Phys.Lett. **B195** (1987) 603; *D.O.Caldwell et al.* Phys.Rev. Lett. **61**; *D.Reusser et al.* Phys. Lett. **B255** (1991) 143; *M.Beck et al.* Phys. Lett. **B336** (1994) 141; *M.Sarsa et al.* Nucl.Phys. (Proc.Suppl.) **B35** (1994) 154.
- [35] *D.Fargion, M.Yu.Khlopov, R.V.Konoplich, R.Mignani.* Phys.Rev. **D54** (1996) 4684.

Appendix.

Differential cross section

$$\frac{d\sigma}{d \cos \theta} = \frac{\beta_f}{32\pi s \beta_\nu} \overline{|M|^2}$$

Definitions

$$\begin{aligned} g_V &= g_A - 4e_f \sin^2 \theta_W \\ G_F &= \pi \alpha_{em} / (\sqrt{2} m_W^2 \sin^2 \theta_W) \\ D_Z &= 1 / [(s - m_Z^2)^2 + m_Z^2 \Gamma_Z^2] \\ D_H &= 1 / [(s - m_H^2)^2 + m_H^2 \Gamma_H^2] \\ D_L &= 1 / [m_\nu^2 + m_W^2 - m_L^2 - 2(kp)] \\ \beta_\nu &= \sqrt{1 - 4m_\nu^2/s} \\ \beta_f &= \sqrt{1 - 4m_f^2/s} \\ m_f &- \text{mass of final particle} \\ N_c &- \text{number of colours in final state} \end{aligned}$$

Matrix elements squared

1. Reaction $\nu \bar{\nu} \rightarrow f \bar{f}$

$$\begin{aligned} \overline{|M_{ff}|^2} &= N_c G_F^2 (F_{ZZ} + F_{HH} + F_{ZH}) \\ F_{ZZ} &= 2m_W^4 / \cos^4 \theta_W D_Z \left[(g_V + g_A)^2 (k_1 p)^2 + (g_V - g_A)^2 (kp)^2 + \right. \\ &\quad \left. m_f^2 (g_V^2 - g_A^2) \left(\frac{s}{2} - m_\nu^2 \right) + m_\nu^2 m_f^2 g_A^2 \frac{s}{m_Z^2} \left(\frac{s}{m_Z^2} - 2 \right) \right] \\ F_{HH} &= 2m_\nu^2 m_f^2 (s \beta_\nu \beta_f)^2 D_H \\ F_{ZH} &= 8 \frac{m_W^2}{\cos^2 \theta_W} m_\nu^2 m_f^2 g_V [(kp) - (k_1 p)] D_Z D_H \times \\ &\quad \left[(m_Z^2 - s - \frac{\Gamma_Z^2}{4})(m_H^2 - s - \frac{\Gamma_H^2}{4}) + m_H m_Z \Gamma_H \Gamma_Z \right] \end{aligned}$$

3. Reaction $\nu \bar{\nu} \rightarrow W^+ W^-$

$$\begin{aligned}
\overline{|M_{WW}|^2} &= G_F^2 m_W^4 (F_{ZZ} + F_{LL} + F_{HH} + F_{ZL} + F_{ZH} + F_{HL}) \\
F_{ZZ} &= D_Z \left\{ 8[-(4(kp)(k_1p) + 7(kp)^2 + 7(k_1p)^2) + (kk_1)(-\frac{s}{2} - 7m_W^2)] - \right. \\
&\quad \frac{4}{m_W^2} [2(3m_W^2 - s)(2(kp)(k_1p) - m_W^2(kk_1)) + 2(4m_W^2 - 3s)((k_1p)^2 + (kp)^2 - \\
&\quad (kk_1)(pp_1)) - 4(s - m_W^2)^2(kk_1)] + \\
&\quad \left. 2\left(\frac{s}{m_W^2}\right)^2 [-((kp) - (k_1p))^2 + (kk_1)((pp_1) - m_W^2)] \right\} \\
F_{LL} &= D_L^2 \left\{ 16[-2(m_\nu^2 - (kp))(k_1p) + (kk_1)(m_\nu^2 - m_W^2)] + \right. \\
&\quad \frac{16}{m_W^2} \{ 2(kp)[((k_1p) - (pp_1))(m_\nu^2 - (kp)) + \\
&\quad ((kk_1) - (k_1p))((kp) - m_W^2) - (k_1p)(m_\nu^2 + m_W^2 - 2(kp))] - \\
&\quad m_W^2 [2((kk_1) - (k_1p))(m_\nu^2 - (kp)) - (kk_1)(m_\nu^2 + m_W^2 - 2(kp))] \} + \\
&\quad \frac{4}{m_W^4} \{ 2(kp)[2((kp) - m_W^2)(2(kp)(k_1p) - m_\nu^2(pp_1)) + m_W^2(k_1p)(m_W^2 - m_\nu^2)] - \\
&\quad \left. m_W^2 [2((kp) - m_W^2)(2(kk_1)(kp) - m_\nu^2(k_1p)) + (kk_1)m_W^2(m_W^2 - m_\nu^2)] \right\} \\
F_{ZL} &= 16 D_Z D_L (m_Z^2 - s - \frac{\Gamma_Z^2}{4}) \left\{ \frac{m_\nu^2 s}{2m_Z^2} ((k_1p) - (kp) - \frac{s}{2} + 2m_W^2) + \right. \\
&\quad (kk_1)(-2(pp_1) + 2m_W^2 + 4(k_1p) + 2(kp)) - \\
&\quad (m_\nu^2 - (kp))(4(kp) + 2(k_1p)) - 4(kp)(k_1p) - 2(k_1p)^2 - \\
&\quad \frac{1}{m_W^2} \{ ((k_1p) - (pp_1))[-(kp)^2 - (k_1p)^2 + 2(kp)(k_1p) - \\
&\quad (kk_1)(m_W^2 - (pp_1))] - (kp)[2(k_1p)((kp) + 2(k_1p)) - \\
&\quad (k_1p)(m_W^2 + 2(pp_1)) + (kp)(2m_W^2 + (pp_1)) \\
&\quad - (pp_1)(2(k_1p) + (kp)) - m_\nu^2(2m_W^2 + (pp_1))] + \\
&\quad ((kp) - m_W^2)[(kp)^2 + (k_1p)^2 - 2(kp)(k_1p) - (kk_1)((pp_1) - m_W^2)] + \\
&\quad (kp)[(k_1p)((kp) + \frac{s}{2}) + (kp)((k_1p) + \frac{s}{2}) - \\
&\quad (kk_1)(2m_W^2 + (pp_1)) - m_W^2(\frac{s}{2} + (k_1p))] + \\
&\quad \frac{m_W^2}{2} [(kk_1)(4(k_1p) + 2(kp) - 3(pp_1) + 3m_W^2) + \\
&\quad (m_\nu^2 - (kp))(-5(kp) - (k_1p)) - (k_1p)^2 - 5(kp)(k_1p)] + \\
&\quad (s - m_W^2)[(kk_1)((pp_1) - m_W^2 + 2(kp)) - \frac{s}{2}(m_\nu^2 - (kp)) - \\
&\quad \frac{s}{2}(k_1p)] - \frac{sm_\nu^2 m_W^2}{2m_Z^2} ((kp) - (k_1p) - m_W^2 + (pp_1)) \} + \\
&\quad \frac{1}{2m_W^4} \{ \{ 2(kp)[(kp)^2 + (k_1p)^2 - 2(kp)(k_1p) - m_W^2((kp) - (k_1p)) \\
&\quad - (pp_1)((kk_1) - m_\nu^2)] +
\end{aligned}$$

$$\begin{aligned}
& m_W^2 [(kk_1)(2(kp) + (pp_1) - m_W^2) - \frac{s}{2}(m_\nu^2 - (kp)) - \frac{s}{2}(k_1p)] \{ (s - m_W^2) + \\
& (pp_1) \{ 2(kp) [(kk_1) ((pp_1) - m_W^2) - (kp)^2 - (k_1p)^2 + 2(kp)(k_1p)] - \\
& m_\nu^2 [((kp) - (k_1p))(pp_1) + \frac{s}{2}((pp_1) - m_W^2)] - \\
& m_W^2 [(kk_1)((pp_1) - m_W^2) - (kp)^2 - (k_1p)^2 + 2(kp)(k_1p)] \} \} \\
F_{HH} &= 8m_\nu^2 D_H \left(\frac{s}{2} - 2m_\nu^2 \right) \left[\left(\frac{s}{2m_W^2} \right)^2 - \frac{s}{m_W^2} + 3 \right] \\
F_{HL} &= 8m_\nu^2 D_L D_H (m_H^2 - s - \frac{\Gamma_H^2}{4}) \left\{ -2 \left[\frac{s}{2} - 2m_\nu^2 - (k_1p) + (kp) \right] - \right. \\
& \frac{2}{m_W^2} [((kp) - (k_1p))((k_1p) - (kp) - \frac{s}{2} + m_W^2) - m_W^2 (\frac{s}{2} - 2m_\nu^2)] + \\
& \left. \frac{1}{m_W^2} \left(\frac{s}{2m_W^2} - 1 \right) [((kp) - (k_1p))((kp) - (k_1p) - m_W^2) - (pp_1) (\frac{s}{2} - 2m_\nu^2)] \right\} \\
F_{ZH} &= -16m_\nu^2 D_H D_Z \left[\left(\frac{s}{2m_W^2} \right)^2 - 3 \right] [(kp) - (k_1p)] \times \\
& \left[(m_Z^2 - s - \frac{\Gamma_Z^2}{4})(m_H^2 - s - \frac{\Gamma_H^2}{4}) + m_H m_Z \Gamma_H \Gamma_Z \right]
\end{aligned}$$

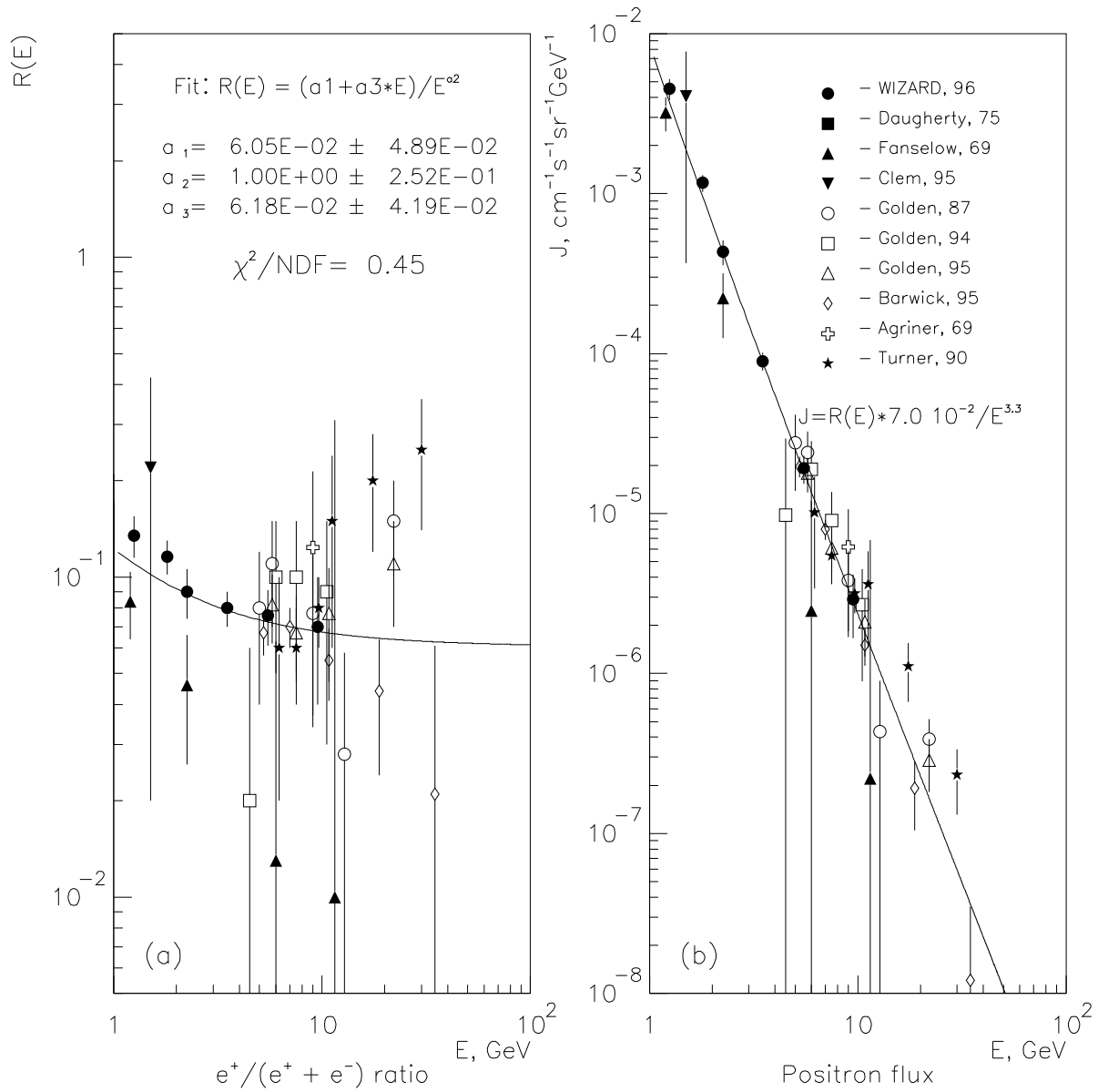


Figure 1: Measured data for the ratio $e^+/(e^+ + e^-)$ (a) and for the positron flux (b) together with the curves resulting from the fit discussed in the text.

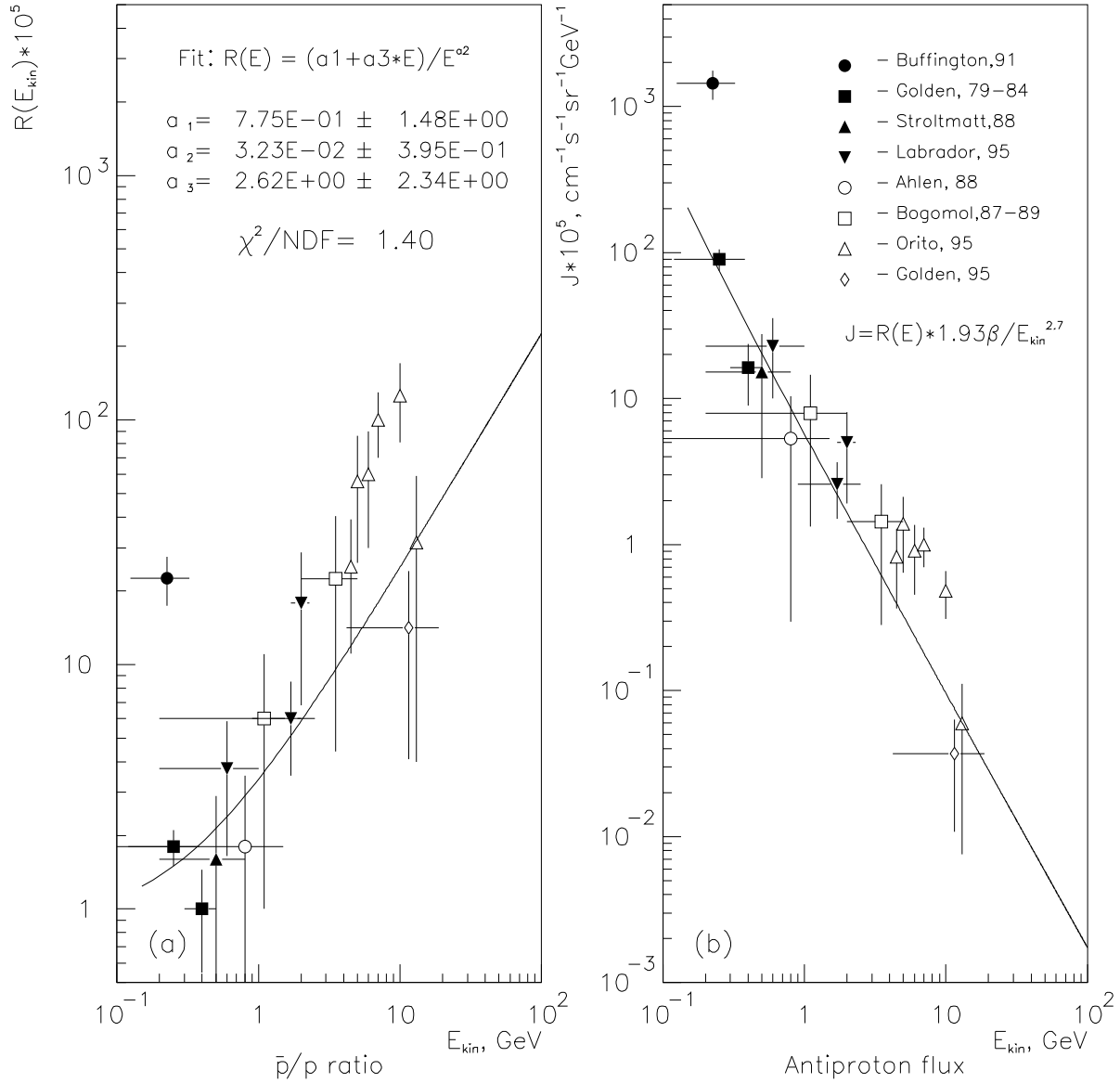


Figure 2: Measured data for the ratio \bar{p}/p (a) and for the antiproton flux (b) together with the curves resulting from the fit discussed in the text.

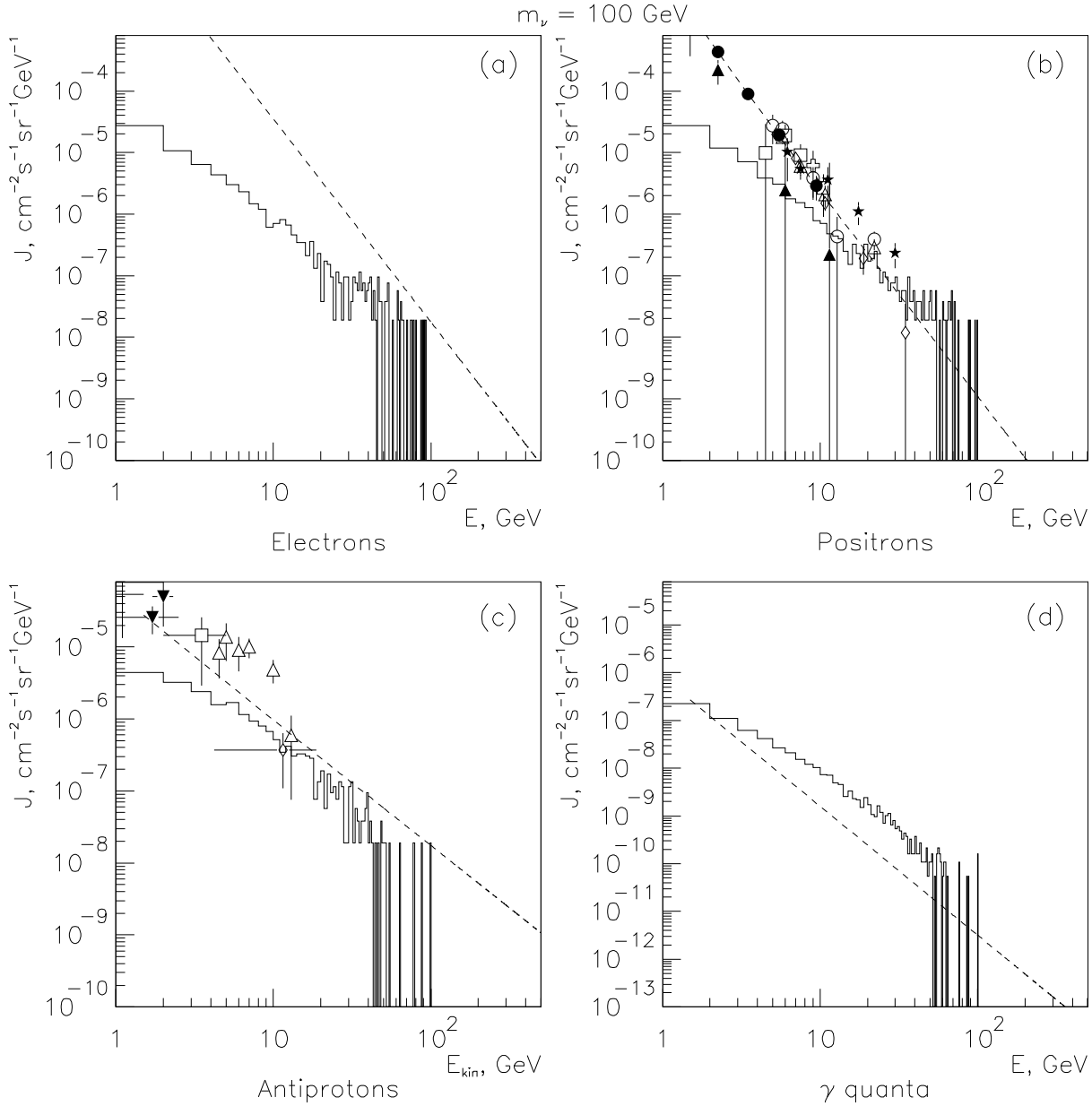


Figure 3: Results of the simulation for $m_\nu = 100 \text{ GeV}$. (a) — electrons; (b) — positrons; (c) — antiprotons and (d) — γ 's. The histograms present the predicted particle fluxes for an energy resolution $\Delta E = 1 \text{ GeV}$. The dashed lines show the observable fluxes for present day experiments (see text).

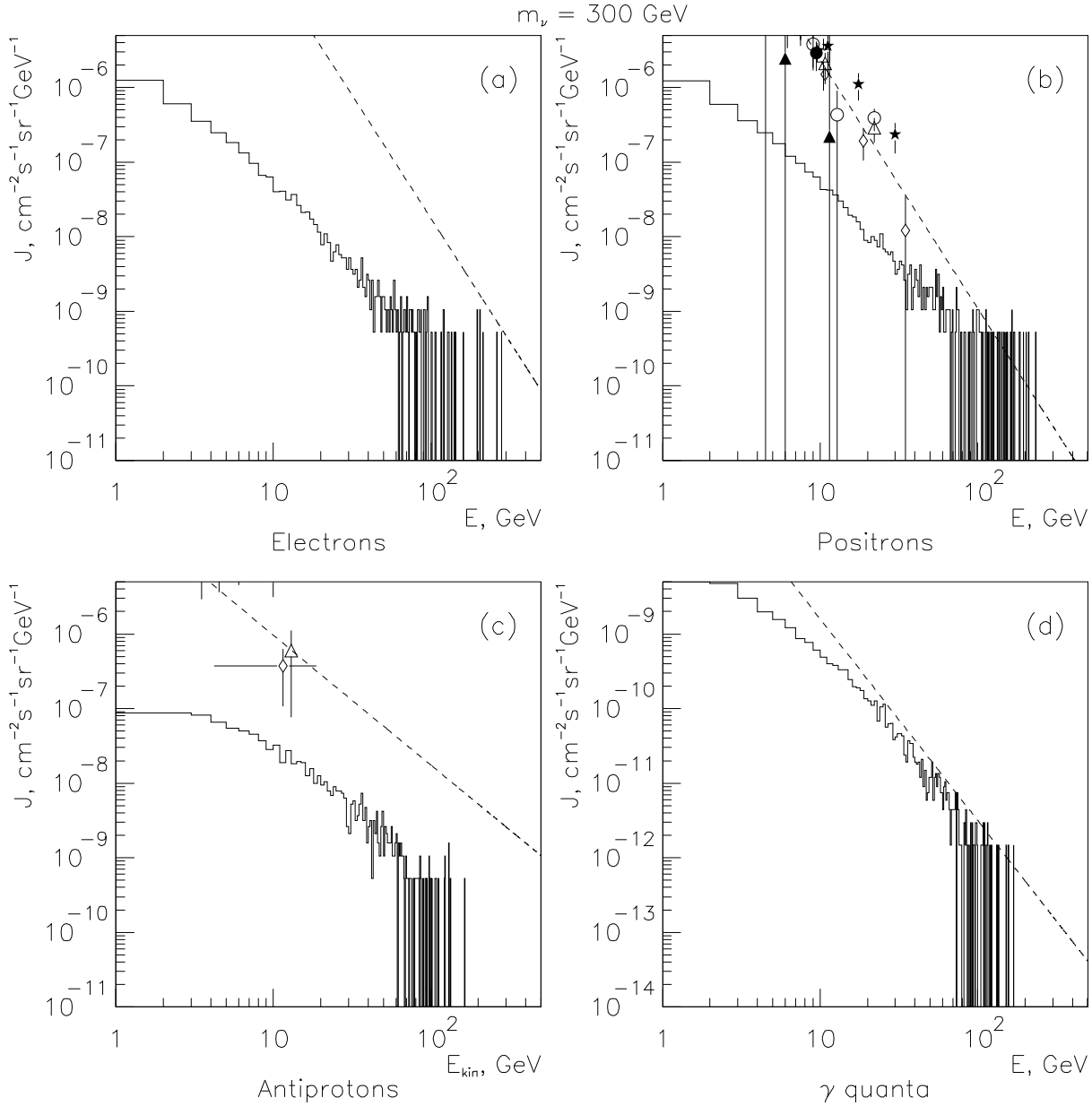


Figure 4: Results of the simulation for $m_\nu = 300 \text{ GeV}$. (a) — electrons; (b) — positrons; (c) — antiprotons and (d) — γ 's. The histograms present the predicted particle fluxes for an energy resolution $\Delta E = 1 \text{ GeV}$. The dashed lines show the observable fluxes for present day experiments (see text).